Effect of Alkyl Properties and Head Groups of Cationic Surfactants on Retention of Cesium by Organoclays

ARTICLE *in* ENVIRONMENTAL SCIENCE AND TECHNOLOGY · JULY 2010

Impact Factor: 5.33 · DOI: 10.1021/es100349k · Source: PubMed

6 AUTHORS, INCLUDING:

Ming-Hsu Li
National Central University
47 PUBLICATIONS **440** CITATIONS

Effect of Alkyl Properties and Head Groups of Cationic Surfactants on Retention of Cesium by Organoclays

TSING-HAI WANG,[†] CHI-JUNG HSIEH,[‡] SHIH-MIN LIN,[‡] DING-CHIANG WU,[†] MING-HSU LI,*[,§] AND SHI-PING TENG[†,∥]

Institute of Nuclear Engineering and Science, National Tsing Hua University, Hsinchu 300, Taiwan, Department of Material Science and Engineering, National Tsing Hua University, Hsinchu 300, Taiwan, Institute of Hydrological and Oceanic Sciences, National Central University, Jhongli, 320, Taiwan, and Radiation Protection Association, Hsinchu, 300, Taiwan

Received February 10, 2010. Revised manuscript received May 23, 2010. Accepted May 25, 2010.

Cationic surfactants modified clays exhibit high sorptive capability toward anionic radionuclides but retention of cationic radionuclides was concurrently reduced. In this study, organoclays were synthesized by intercalating a variety of primary/quaternary alkylammonium species ($NH_2R/(CH_3)_3N^+RBr^-$, where R = benzyl, dodecyl, and octadecyl) into bentonite MX-80. The effect of surfactant's properties on enhancing or limiting cationic sorption capability was investigated by performing Cs sorption experiments. Experimental results were analyzed using the MINEQL+ software by considering Cs uptake by structural and edge sorption sites. Bentonites that were intercalated with primary alkylammonium surfactants had a higher sorptive capacity than those intercalated with quaternary alkylammonium surfactants. Samples intercalated with octadecyl-bearing surfactants had the lowest sorption rate. XRD and FTIR analyses revealed that each organoclay had a characteristic arrangement of alkyl chains. The cation retention of organoclays was dominated by the extent of hydrophobic interactions affected by the local distribution and arrangement of surfactants. The intercalated primary alkylammoniun surfactants tended to transform into local clusters with a high packing density, leaving more structural sites available for Cs uptake. In contrast, the NH_3R^+-surfactants tended to form a denser monolayer over clay surface, inhibiting the retention of Cs at structural sites.

Introduction

Clay minerals have numerous industrial applications, including as chemical catalysts and adsorbents for hazardous contaminants. Montmorillonite, which is the major clay constituent of bentonite, is adopted extensively in adsorbent applications because of its favorable properties, which include high surface area, high swelling capacity, and high sorption capacity toward cationic contaminants. Montmorillonite is a member of dioctahedral smectites with an aluminum octahedral sheet sandwiched by siloxane tetrahedral sheets. Isomorphic substitution causes montmorillonite to bear negative charges, which make it an effective adsorbent for cationic contaminants and a suitable buffer material for use in radioactive waste repositories (*1, 2*). Repository facilities are likely to release not only cationic nuclides (Cs-137, Sr-90, Co-60) but also anionic ones (Se-79, Tc-99, I-129), but the retention of anionic nuclides by clay minerals is greatly limited due to electrostatic repulsion. The ability of clays to adsorb anionic nuclides can be improved by surface modification by covering it with either iron oxides or organic surfactants (*3*−*6*).

Organoclays are synthesized by intercalating cationic surfactants into interlayer spaces through cation exchange. The surface properties of the organoclays thus obtained strongly depend on the nature of the intercalated surfactants (*7*). The alkyl moiety of intercalated surfactants inside the clay interlayer behaves as an analogous bulk organic phase, making organoclays effective for remediating environments that are contaminated by organic compounds (*8, 9*). The adsorption of solution organics by organoclays straightforwardly reduces the probability of ligand-mediated nuclide transport. Besides adsorbing organic contaminants, organoclays are capable of adsorbing anionic ions (*4*−*6, 10*). Although the uptake of anionic nuclides by organoclays can be technically achieved, the ability of organoclays to retain cationic nuclides is greatly reduced concurrently (*4*−*6*). This trade-off is attributed to the variations of organoclays' surface properties, which are closely related to the concentration of surfactants applied and the arrangement of surfactants within the clay sheets (*11*−*13*).

In this study, we investigate the effect of alky properties and head groups of cationic surfactants on the retention of cesium, a critical radionuclide considered in the safety assessment of radioactive waste repositories, by organoclays synthesized with a variety of primary/quaternary alkylammonium surfactants. Results of Cs sorption experiments were fitted by a chemical equilibrium modeling system, MINEQL+, to distinguish contributions of Cs uptake by structural and edge sorption sites. Surface properties of surfactant-modified bentonite MX-80 were analyzed with Brunauer−Emmett−Teller (BET), X-ray diffraction (XRD), and Fourier transform infrared spectra (FTIR) to support our findings.

Material and Methods

Materials. Commercially available bentonite MX-80 (herein MX-80) was used in this study. It is a Na-bentonite with mineral compounds including montmorillonite (75.5 wt %), quartz (15 wt %), and other minor minerals such as feldspars (5−8 wt %) and mica (<1 wt %). Ninety wt% of the grain sizes of MX-80 are smaller than 20 μm. The cation exchange capacity (CEC) of MX-80 is 76 $cmol_c\ kg^{-1}$ and its chemical composition is 60.25% SiO_2, 19.61% Al_2O_3, 3.75% Fe_2O_3, 0.13% FeO, 2.38% MgO, 1.83% CaO, 0.03% Na_2O, and 0.10% K_2O. The half structural formula of the montmorillonite fraction of MX-80 is $(Si_{3.96}Al_{0.04})$-$(Al_{1.55}Fe^{3+}_{0.20}Fe^{2+}_{0.01}Mg_{0.24})O_{10}(OH)_2Na_{0.30}$ (*14*). The surfactants applied herein were benzylamine ($C_7H_7NH_2$, Bamine), dodecylamine ($C_{12}H_{25}NH_2$, DDamine), octadecylamine ($C_{18}H_{37}NH_2$, ODamine), benzyltrimethylammonium bromide ($C_7H_{10}NBr$, BTMA), dodecyltrimethylammonium bromide ($C_{15}H_{34}NBr$, DDTMA), and octadecyltrimethylammonium bromide ($C_{21}H_{46}NBr$, ODTMA) from Sigma-Aldrich. The other chemicals used—CsCl, NaCl, ethanol, HCl, and NaOH—were of analytical grade and also obtained from Sigma-Aldrich.

* Corresponding author phone: +886-3-4222964; fax: +886-3-4222964; e-mail: mli@cc.ncu.edu.tw.
[†] Institute of Nuclear Engineering and Science, National Tsing Hua University.
[‡] Department of Material Science and Engineering, National Tsing Hua University.
[§] National Central University.
[∥] Radiation Protection Association.

10.1021/es100349k

Published on Web 06/10/2010

Preparation. Organoclays were synthesized as follows: (1) disperse 20 g of MX-80 in 2 L of deionized water in a 5-L double-necked reaction bottle with vigorous stirring; (2) add surfactants in a stoichiometric amount equivalent to 1.0 CEC into clay suspensions; (3) add a total of 200−300 mL of ethanol into a clay/surfactant mixture to enhance the dissolution of organic surfactants; (4) continue to stir the mixtures vigorously at 60 °C for 24 h to evaporate the ethanol slowly; (5) collect the organoclays by centrifuging at 15 000 rpm for 15 min; (6) wash the obtained organoclays several times using deionized water until the $AgNO_3$ test is passed; (7) dry the obtained organoclays at 60 °C under reduced pressure; grind them manually in an agate mortar; collect samples with grain size <0.25 mm using a sieve; and then store samples at 60 °C under reduced pressure before use to minimize the influence of environmental humidity.

Sorption Experiments. For the Cs sorption experiments, 10.0 g of synthesized organoclays was dispersed in 1.0 L of 0.1% wt NaCl background electrolyte (I = 0.017 M) in a double-necked bottle. The concentration of Cs^+ was 100 ppm (7.5×10^{-4} mol/L). The high Cs concentration and low solid/liquid ratio reduce the effect of surface heterogeneity of bentonite MX-80. The initial pH of the mixtures was adjusted to acidic (pH 2.0−2.5) by adding 1.0 M HCl. After 24 h of continuous stirring, 1 mL of supernatant of mixtures was extracted using a syringe with a stainless needle. The pH of the remaining mixture was recorded and then adjusted by adding 1.0 M NaOH solution dropwise, and then stirring for another 24 h and collecting 1 mL of supernatant again. The sampling cycle was repeated until collected samples reach alkaline (pH 11.5−12.0). Sampled supernatants were individually filtered (using a 0.45-μm Millipore filter cell), diluted with 1% wt HNO_3 solutions, and then introduced to an ethylene−air flame atomic absorption spectrometer (Varian SpectrAA-30) to determine the concentration of Cs. The differences in Cs concentrations were interpreted to be the amount of Cs adsorbed. The sorption experiments were conducted in triplicate using clay samples from different batches.

Modeling. To quantitatively evaluate sorption capability of organoclays, results from sorption experiments were fitted using MINEQL+ version 4.6 with the two-layer model. MINEQL+ is a chemical equilibrium modeling system combining the WATEQ3 thermodynamic database and the numerical structure of MINEQL (*15*). The two-layer model consists of one surface layer and one layer of diffusion ions. Surface potential is calculated from the net surface charge according to the Gouy−Chapman theory. The uptake of Cs is assumed to occur at structural sites by ion exchange and at edge sites by surface complexation with the two-layer model. The sorption of Cs at structural sites are given by

$$\equiv X\mathrm{Na} + \mathrm{Cs}^+ \leftrightarrow \equiv X\mathrm{Cs} + \mathrm{Na}^+, \qquad K_x = \frac{[\equiv X\mathrm{Cs}][\mathrm{Na}^+]}{[\equiv X\mathrm{Na}][\mathrm{Cs}^+]} \quad (1)$$

where $\equiv X$ is the amount of structural sorption sites (mol/L), which equals $\equiv X$Na and is identical to its CEC value (7.6×10^{-3} mol/g). $[Cs^+]$ and $[Na^+]$ are concentrations (mol/L) of Cs^+ and Na^+, respectively. K_x is the equilibrium constant of the ion exchange reaction.

The edge sorption sites are pH-dependent and the following protonation/deprotonation reaction is considered.

$$\equiv \mathrm{SOH}_2^+ \leftrightarrow \equiv \mathrm{SOH} + \mathrm{H}^+, \qquad K_{a1} = \frac{[\equiv \mathrm{SOH}][\mathrm{H}^+]}{[\equiv \mathrm{SOH}_2^+]} \exp\left(-\frac{F\psi}{RT}\right) \quad (2)$$

$$\equiv \mathrm{SO}^- + \mathrm{H}^+ \leftrightarrow \equiv \mathrm{SOH}, \qquad K_{a2} = \frac{[\equiv \mathrm{SOH}]}{[\equiv \mathrm{SO}^-][\mathrm{H}^+]} \exp\left(-\frac{F\psi}{RT}\right) \quad (3)$$

where $\equiv \mathrm{SOH}_2^+$, $\equiv$ SOH, and $\equiv \mathrm{SO}^-$ refer to the positively charged, neutral, and negatively charged edge sites, respectively, and K_{a1} ($10^{10.5}$) and K_{a2} ($10^{8.5}$) are the intrinsic equilibrium acidity constants, which are determined by potentiometric titrations conducted under identical experimental conditions (with 1.0 g of clay dispersed in 100 mL of 0.1 wt % NaCl solution). The exponential term is the Coulombic correction factor, which is associated with the electrostatic effect (*16*).

The retention of cesium at edge sorption sites is given by

$$\equiv \mathrm{SOH} + \mathrm{Cs}^+ \leftrightarrow \equiv \mathrm{SOCs} + \mathrm{H}^+, \qquad K_s = \frac{[\equiv \mathrm{SOCs}][\mathrm{H}^+]}{[\equiv \mathrm{SOH}][\mathrm{Cs}^+]} \exp\left(-\frac{F\psi}{RT}\right) \quad (4)$$

where K_s is the equilibrium constant. The concentration of $\equiv$ SOH (4.0×10^{-4} mol/g) is taken from the literature, using a model of {110}, {100}, and {010} edge face structures (*17*). The experimental curves were best-fitted by trial-and-error. To keep the modeling results tractable, any reaction that did not improve the fitting was discarded.

Characterization. The BET specific surface area, mean width of pores, and volume of micropores were computed from N_2 adsorption isotherms using a Micromeritics ASAP2020 sorptometer at 77 K. Raw and surfactant-modified MX-80 samples were degassed at 105 °C until a steady interior pressure <10 μmHg was reached. N_2−BET measurements were then made. Specimens of raw/surfactant-modified MX-80 were prepared for XRD analyses by spraying powdered clay/organoclay over the sample holder with a random orientation and smoothing contact surface. The XRD patterns were recorded using Cu Kα_1 radiation (λ = 0.15406 nm) on a Shimadzu XRD 6000 diffractometer equipped with a counter monochromator that was operated at 30 kV and 20 mA between 2 and 10° (2θ) at a scan rate of 4° (2θ) per minute. The dried clay/organoclays specimens were prepared by dispersing 1.0 mg of clay into 10.0 mg of KBr and pressing the resulting material into a transparent disk for FTIR analyses (Bomen DA8.3). FTIR spectra were obtained over the spectral range of 620−4000 cm^{-1} with a total of 200 scans with a resolution of 4 cm^{-1}. Wet samples that were gathered at the end of the sorption experiments were analyzed by ATR-FTIR using a Nicolet Magna 860 spectrometer at beamline 14A1 at the National Synchrotron Radiation Research Center (NSRRC), Taiwan. To acquire the ATR-FTIR spectra, a suitable amount of wet paste was paved uniformly over the ZnSe ATR cell. The ATR-FTIR spectra were recorded using a liquid nitrogen-cooled MCT/A detector over the range 620−4000 cm^{-1} with a total of 640 scans with a resolution of 4 cm^{-1}.

Results and Discussion

Sorption Study. Figure 1 shows the amount of cesium adsorbed by raw/surfactant-intercalated MX-80 under various pH environments. Three distinct sorption characteristics were observed: Bamine-, DDamine-, and ODamine-modified samples had the highest Cs sorption capabilities (Group I); BTMA-modified samples (Group II) exhibited Cs retention similar to that of raw MX-80; DDTMA- and ODTMA-modified samples (Group III) exhibited the lowest Cs sorption.

To facilitate fitting by the MINEQL+, the following assumptions were made: (a) The structural ($\equiv X$) and edge sorption sites ($\equiv$ SOH) on clay surfaces contribute to the retention of Cs. (b) The Cs sorption by edge sites is pH-dependent, while no proton uptake occurs at structural sites. This assumption is reasonable because proton uptake by structural sites occurs only in acidic environments with very

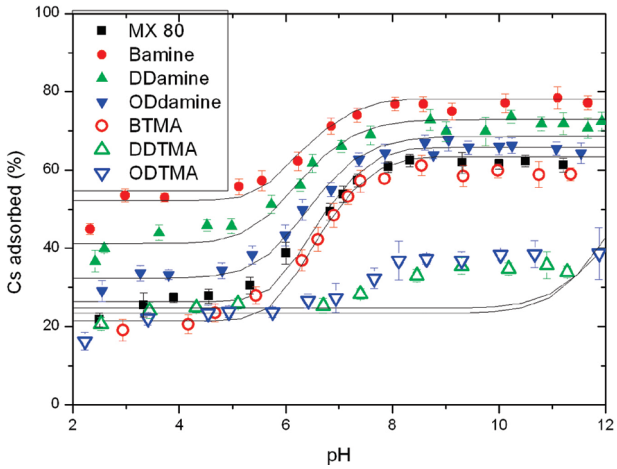

FIGURE 1. Experimental and fitting results of cesium sorption to raw/surfactant-intercalated clay samples.

TABLE 1. log *K* values of Cesium Sorption by Structural and Edge Sites

samples	log K_x at structural sites	log K_s at edge sites
MX-80	0.32	−2.3
BTMA	0.20	−2.5
DDTMA	0.28	−8.5
ODTMA	0.25	−8.5
Bamine	0.82	−1.8
DDamine	0.62	−2.5
ODamine	0.45	−2.8

low ionic strength ($I < 0.001$ M) (*18*). (c) All replaceable Na ions of raw MX-80 are exchanged by surfactant molecules (such that the identical concentration of structural sorption sites after intercalation equals that before). Therefore, all reactive structural sites on the surfaces of organoclays become ≡ Suf, and all are active toward Cs^+. This assumption is supported by observations of complete intercalation when the cationic surfactants loading is equivalent to 1.0 CEC (*6, 19, 20*). (d) Although significant structural variations are observed after modification, we ignore the effect of intercalation on surface potential. The same assumption holds for the protonation/deprotonation of edge sorption sites. The variation in surface potential of edge sites caused by surfactant intercalation is reflected in differences of sorption capability toward Cs ions.

The best-fitted curves and the resulting log *K* are shown in Figure 1 and Table 1, respectively. Group I samples have higher log K_x values (0.45 for ODamine, 0.62 for DDamine, and 0.82 for Bamine) than those of other samples; samples of BTMA, DDTMA, and ODTMA exhibited lower log K_x values than that of raw MX-80. Based on the fitting results, structural sites dominate the Cs uptake under acidic conditions while edge sorption sites are responsible for Cs sorption in alkaline environments (Figure 2). Because all structural sites of organoclays are occupied by surfactant molecules, a higher log K_x means more incorporated surfactants to actively participate in Cs sorption (exchange). Accordingly, the higher log K_x of organoclays than that of raw MX-80 also indicates that binding forces between primary amine species and structural sites are weaker than those between Na ions and structural sites. By contrast, modification using quaternary ammonium surfactants (Group II and III) significantly reduces log K_x, reflecting the opposite binding tendency to those of Group I samples. This observation suggests that the binding forces between surfactants and structural sites of MX-80 deceases in the order Cs^+ > DDTMA≈ ODTMA > BTMA> Na^+> ODamine> DDamine> Bamine.

At edge sites, only modification by Bamine species increases the log K_s of organoclays. Furthermore, finding an appropriate log K_s that precisely describes the sorption features in alkaline environments becomes difficult (Figure 2). A lower log K_s implies that fewer edge sites can participate in Cs uptake. Because no surfactant is expected to be incorporated onto edge sites, the decrease in log K_s may be explained by the action of intercalated surfactants as hydrophobic spacers, restricting access of aqueous Cs ions to the edge sites. Incorporated surfactants modify the surface charges of montmorillonite, according to zeta potential measurements (*21*) and so may deactivate edge sorption sites.

BET, XRD, and FTIR studies. Intercalated-surfactant modification greatly reduces the specific surface areas (S_a in Table 2), especially those of the ODTMA-, DDamine-, and ODamine-modified samples. The decreased S_a is a consequence of the disappearance of micropores, which is caused by the blocking of the N_2 passage by intercalated surfactants, leaving only a small fraction of the interlamellar pores accessible (*13, 22*). Increased average pore width from ca. 6.71 to 16−19 nm is observed along with the decrease in micropore volume. The measured surface area of clay minerals is the sum of the surface areas of the interlayer spaces (micropores), the interparticle spaces (micro/mesopores inside the assembly of silicate layers), and the interaggregate spaces (meso/macropores inside the assembly of particles) (*13*). Accordingly, the disappearance of micropores suggested that the surfactants are intercalated into the interlayer spaces of MX-80, rather than being adsorbed/precipitated to/in interparticle and interaggregate spaces.

Figure 3a presents the XRD patterns of raw and surfactant-intercalated MX-80. The raw MX-80 sample has a *d*-space of 0.99 nm, corresponding to dehydrated Na-montmorillonite (*23*); while the *d* spaces of organoclays expand significantly after modification. This clearly indicates the intercalated surfactant molecules into the interlayer of MX-80 and is in good agreement with BET observations of the disappearance of micropores. For benzyl-surfactants intercalated organoclays, their interlayer places are expanded by 0.43 nm (BTMA) and 0.40 nm (Bamine), respectively. The moiety of the benzyl substitute, like the benzene molecule itself, is a flat molecule with a thickness of about 0.4 nm and a length of 0.66 nm, whereas the cross-sectional diameter of the alkyl chain is ca. 0.46 nm (*24*). The expansion of around 0.40 nm may be caused by the orientation of benzyl and alkyl chains parallel to the clay surfaces in a monolayer arrangement (*7, 25*). The slightly smaller expansion of Bamine samples than that of BTMA ones might be attributed to the fact that the head groups of Bamine (benzyl-NH_3^+) form hydrogen bonds with oxygen in the silicate surfaces (*7*). Under these conditions, each of the three H atoms of Bamine can reach the oxygen atom in the superficial cavity and the thus attract Bamine species closer to the clay surfaces (*7*).

When MX-80 is intercalated with dodecyl substitute surfactants, *d*-spaces of 1.41 and 1.54 nm are observed for DDTMA and DDamine samples, respectively. This corresponds to the expansion about 0.54 nm for the DDamine samples, suggesting that the dodecyl chains of DDamine surfactants lie flat on the silicate surfaces with a monolayer arrangement. When surfactants with octadecyl substitute are intercalated, a $d_{(001)}$ value of about 1.82 nm is obtained (0.82 nm of expansion). The 0.82 nm expansion is several times the thickness of the cross-section of the alkyl chains (*7*). Accordingly the intercalated ODamine and ODTMA species are reasonably expected to be oriented in bilayer arrangements.

The intercalated amines exhibit significantly broadened d_{001} diffraction peaks, especially in the cases of ODamine-intercalated MX-80. The broadening in the diffractograph is caused by the superimposition of reflections where the orientation of alkyl chains inside *d*-spacing possesses at least

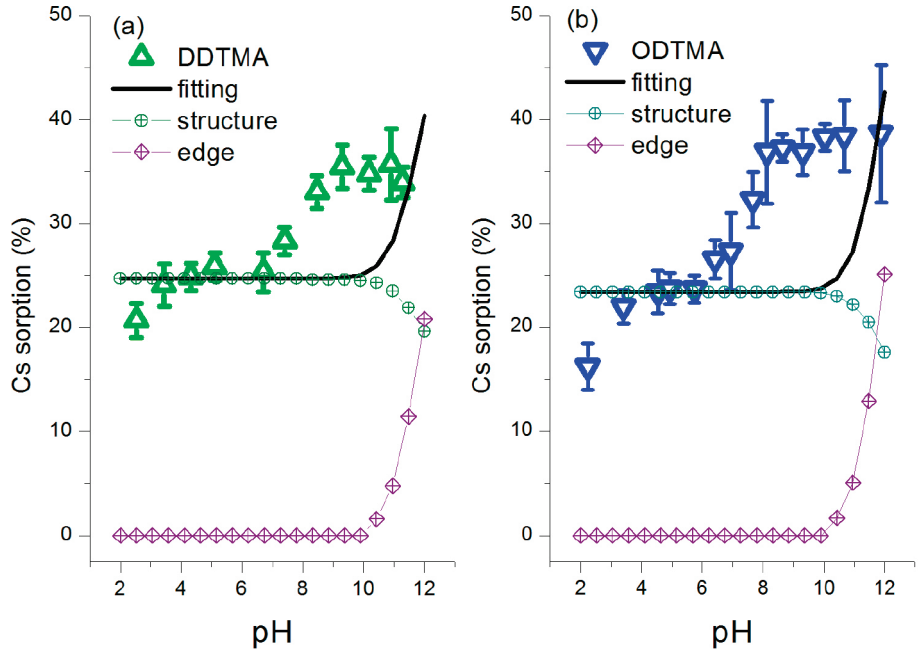

FIGURE 2. Fitting result of Cs sorption to (a) DDTMA- and (b) ODTMA-intercalated clay samples. In the legend, structure stands for Cs sorption by structure sites and edge means the Cs uptake by edge sorption sites.

TABLE 2. Surface Properties of Raw and Surfactant-Intercalated Clay Samples Measured by N_2—BET Method[a]

sample	BET specific surface (m^2/g)	average pore width (4 V/A by BET)(nm)	micropore volume (*t*-plot method)($\times 10^{-4}$ cm^3/g)	micropore area (*t*-plot method)(m^2/g)
MX80	36.98	6.71	83.83	18.23
BTMA	26.50	6.69	36.96	8.54
DDTMA	14.06	16.19	14.65	3.49
ODTMA	6.17	18.78	3.49	0.93
Bamine	28.93	5.78	56.26	12.55
DDamine	2.71	24.46	5.15	1.23
ODamine	1.99	19.78	3.36	0.84

[a] The experimental error during surface area determination was evaluated by triplicating N_2-BET measurements with Micromeritics ASAP2020 sorptometer and <5%.

two kinds of arrangements. A linear combination of two Gaussian functions is used to fit this d_{001} diffraction (~2.5−6.0, $2\theta°$), indicating that the d_{001} diffraction of ODamine samples consists of diffraction from basal spaces of 2.88 and 1.89 nm, respectively. The former one corresponds to expansion by 1.88 nm, while the latter indicates the expansion by 0.89 nm. The expansion by 0.89 nm could be attributed to the bilayer orientation of octadecylamines within the interlayer spaces. However, the expansion by 1.88 nm is difficult to explain. If the pseudotrimolecular layer arrangement of the octadecylamine were to emerge, then the *d*-space would be expanded by ~1.2 nm, not by 1.88 nm. One possible cause of the 1.88 nm expansion may be attributed to diffraction effect. Contributions to this expansion by the Lorentz-Polarization factor may be responsible for the systematic shifting of diffraction peaks toward low angles and, therefore overestimation of the actual layer thickness (*26*). Nevertheless, it is certain that the orientation of alkyl chains of intercalated surfactants, especially intercalated primary alkylammonium surfactants, is not uniformly distributed over clay surfaces.

The solid lines in Figure 4 represent the FTIR spectra that were obtained from dried samples while the dotted lines are the ATR-FTIR spectra of wet samples obtained at the end of sorption experiments. Since weighing wet pastes is practically difficult, they were not weighed and the difference between the absorption intensities of the dry and wet samples can only be discussed quantitatively. The IR-active modes in the wavenumber region between 2700 and 3100 are the asymmetric (υ_{as}) and symmetric (υ_s) stretching vibration of the methylene moiety of the surfactants. This is sensitive to changes in the gauche/trans conformer ratio and the lateral chain−chain interactions (*20*). Bamine and BTMA samples yielded no significant symmetric or asymmetric stretching vibrations of methylene, because for the benzyl substitute CH_2 vibrations are not dominant modes. DDTMA samples exhibit only weak υ_s and υ_{as} stretching following Cs sorption experiments, whereas they exhibit intense absorptions in the dry state. The frequencies of both symmetric and asymmetric CH_2 stretching shift downward to lower frequencies, suggesting the transformation of alkyl chains from disordered conformations to more trans-conformations with a simultaneous increase in the packing density of the alkyl chains (*20*). The significant decrease in absorption intensity herein may be related to the fact that intercalated surfactant molecules are exchanged by Cs ions, while the shift in wavenumbers may be attributed to rearrangement of the alkyl chains during the sorption experiments.

For DDamine samples, the decrease in absorption intensities after the sorption experiments is not as significant as that of DDTMA samples, indicating more DDamine surfactants remained after Cs sorption. The concurrent downward shift in both symmetric and asymmetric CH_2 stretching after Cs sorption indicates that the interlayer alkyl chains are rearranged, increasing their packing density. The interlayer alkyl chains of MX-80 intercalated by octadecyl-bearing surfactants have a denser arrangement than the other

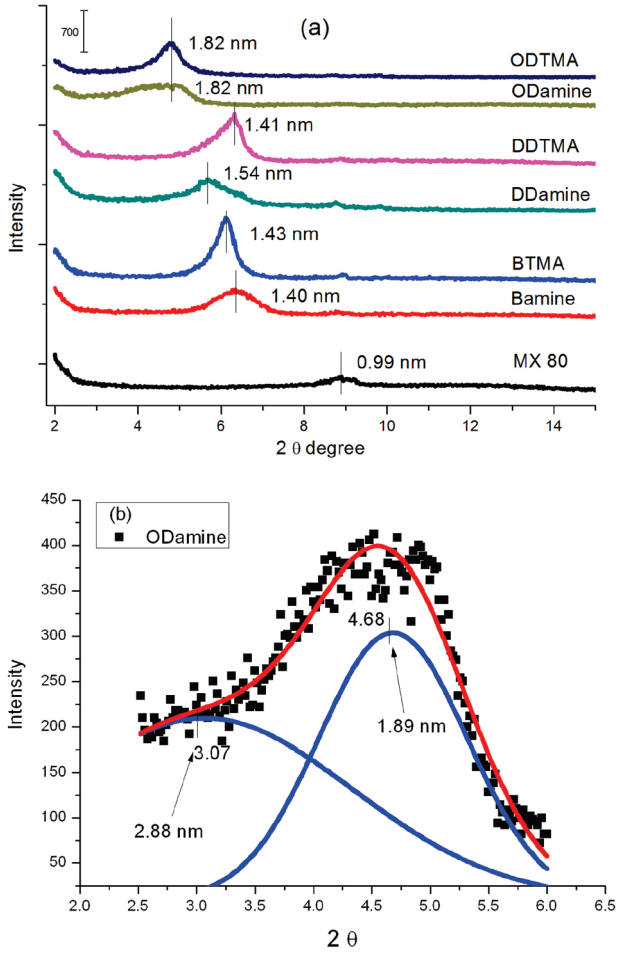

FIGURE 3. (a) XRD patterns of raw and surfactant-intercalated clay samples, (b) d_{001} diffraction fitted by superposition of two Gaussian distributions. Fitting is achieved by using the OriginPro 8 software (OriginLab Corporation, USA). The deduced expansion by 1.88 nm (2.88 nm shown in the figure) is used to account for the arrangement of intercalated octadecylamine. Samples for XRD analyses were stored at 60 °C under reduced pressure before measurement.

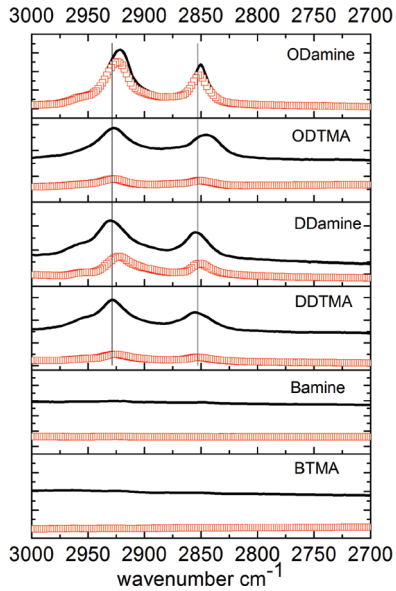

FIGURE 4. FTIR spectra of surfactant-intercalated clay samples before (solid lines) and after Cs sorption experiments (dotted lines).

surfactants as suggested by their lower frequencies of both symmetric and asymmetric CH_2 stretching. The absorption intensity of ODTMA is greatly reduced after the sorption experiments while that of the ODamine samples is independent of whether they are in the dry or wet states. The shift of the asymmetric CH_2 absorption modes exceeds that of the symmetric CH_2 modes, suggesting that the symmetric CH_2 stretching absorption mode is less sensitive to variations in conformation than is the asymmetric CH_2 stretching absorption mode (*27*).

Mechanism of Cs Sorption onto Organoclays. Instinctively, retention of Cs should be enhanced as modified organoclays having higher surface areas. However, this claim contradicts observations made herein: while the surface areas of amine-modified samples are greatly reduced (Table 2), those samples present a higher Cs uptake than those of raw and quaternary alkyammonium-modified ones (Figure 1). Since surface areas were determined by the BET in the dried stage, the available surface areas are believed to be quite different in aqueous environments where Cs sorption experiments were performed.

When in dried stage, intercalated surfactants inside organoclays adopt monolayer/bilayer formations with their alkyl chains parallel to the clay surfaces. Such arrangement prevents access by gaseous N_2 molecules and explains the observed small surface areas (*13*). However, once surfactant-intercalated samples are dispersed into solutions that contain Cs cations, cation exchange reactions occur and the intercalated surfactant molecules are gradually exchanged. The organic layers that were able to restrict access by gaseous N_2 become discontinuous and the interrupted surfactants are forced to rearrange into clusters, increasing packing density. Although intercalation transforms the clay surfaces from hydrophilic to hydrophobic (*11*), preventing access by aqueous ions due to phase separation, the strong hydration between ammonium heads group and counterions (Cl^- in this study) will cause water and Cs ions to enter the surfactants arrangements and weaken hydrophobicity (*20*). Hence, the extent of Cs uptake by organoclays was determined by the balance between cation exchanges and hydrophobic interactions.

Although head groups with NH_3^+-R of alkylammonium surfactants have additional hydrogen bonds toward clay surfaces compared to $(CH_3)_3N^+$-R heads (*7*), the former can also form hydrogen bonds with water molecules as well as chloride anions. Therefore, hydrated NH_3^+-R heads are more effective in bringing water molecules and Cs ions into surfactants arrangements than are $(CH_3)_3N^+$-R heads, and support the observations that samples intercalated by primary alkylammonium surfactants have a higher Cs uptake than others.

Intercalated Bamine and BTMA species expand the basal spaces of clay particles, which provoke more sorption sites available for Cs ions. The hydrophobic interactions between benzyl chains of intercalated Bamine/BTMA species are the weakest of those among the surfactants used herein; making associated surface organic layers highly vulnerable to access by water/Cs molecules. As a result, BTMA samples have Cs sorption similar to that of raw MX-80, while the Bamine samples exhibit a higher Cs uptake owing to their head groups. The chemical details of the headgroup and the chains of the surfactants are closely related to the functionality of organoclays, but they do not significantly affect the relationship between packing density and the molecular ordering of the intercalated surfactants (*7*). This argument explains the similarity between the absorption frequencies of symmetric and asymmetric CH_2 stretching observed in FTIR spectra from samples intercalated with dodecyl- and octadecyl-surfactants (Figure 4). Because the octadecyl substitute has six more carbons in the alkyl chains than that of the dodecyl substitute, more hydrophobicity is introduced and less Cs

sorption is observed when the octadecylammonium is used. To accommodate the additional alkyl moiety in the confined interlayers, the interlayers are expanded and the octadecyl alkyl chains are oriented into a bilayer arrangement. When dodecyl- and octadecyl-modified organoclays are dispersed in aqueous systems, the surfactant alkyl chains are driven into closer contact and the intercalated surfactant molecules are transformed from dispersed monomers to aggregate clusters upon wetting (*20*), reflecting a much more profound downward shift as observed in FTIR spectra (Figure 4).

The broadened peak of ODamine (Figure 3b) indicates the coexistence of various arrangements and of mixed-layer arrangements (*11*). The amount of exchangeable surfactants will vary substantially with the local arrangement of alkyl chains. Weakly bound surfactant molecules can be exchanged for Cs, while the strongly bound ones will not be exchanged but remain inside galleries. The remaining surfactant molecules undergo rearrangement to minimize the contact area of their surfaces with the aqueous environments, leading to the formation of densely packed aggregates or clusters of surfactants (*25*). Simultaneously, hydrophobic interactions between alkyl chains of intercalated (on clay surfaces) and exchanged (in solutions) surfactants introduce further cationic surfactants and cations into clay interlayers (*20*). This phenomenon explains the similar absorption intensities in the FTIR spectra of ODamine samples before and after Cs sorption. Additionally, the bulky methyl groups on head groups of the quaternary surfactant serve as spacers that keep the cationic N center away from the MX-80 surfaces, leading to a flexible orientation of the R-NMe_3^+ headgroup on the clay surface (*7*). This orientation makes clay surfaces more hydrophobic, inhibiting access by Cs ions and explaining the lower Cs uptake by samples intercalated by the quaternary alkylammonium surfactant. In contrast, the strong hydration of ammonium heads and the aqueous counterions, such as the Cl^- anions of background electrolytes, weakens the hydrophobicity of clay surfaces and thus increase the Cs sorption capacities (*20*). By rearranging alkyl chains toward denser local organic clusters, organoclays can adsorb more cations through their hydrophobic surfaces.

Acknowledgments

This study was funded by the Atomic Energy Council and the Nation Science Council of Taiwan through projects NSC97-NU-7-007-004 and NSC97-2221-E-007-066-MY3. We are grateful to Dr. Yao-Chang Lee for access to beamline 14A1 in the National Synchrotron Radiation Research Center. Ted Kony is appreciated for his editorial assistance.

Literature Cited

(1) Wu, T.; Amayri, S.; Drebert, J.; Van Loon, L. R.; Reich, T. Neptunium(V) sorption and diffusion in opalinus clay. *Environ. Sci. Technol.* **2009**, *43*, 6567–6571.
(2) Wang, T. H.; Li, M. H.; Yeh, W. C.; Wei, Y. Y.; Teng, S. P. Removal of cesium ions from aqueous solution by adsorption onto local Taiwan laterite. *J. Hazard. Mater.* **2008**, *160*, 638–642.
(3) Jan, Y. L.; Wang, T. H.; Li, M. H.; Tsai, S. C.; Wei, Y. Y.; Teng, S. P. Adsorption of Se species on crushed granite: A direct linkage with its internal iron-related minerals. *Appl. Radiat. Isot.* **2008**, *66*, 14–23.
(4) Bors, J.; Gorny, A.; Dultz, S. Iodide, cesium and strontium adsorption by organophilic vermiculite. *Clay Miner.* **1997**, *32*, 21–28.
(5) Bors, J.; Dultz, S.; Riebe, B. Retention of radionuclides by organophilic bentonite. *Eng. Geol.* **1999**, *54*, 195–206.
(6) Dulz, S.; Bors, J. Organophilic bentonites as adsorbents for radionuclides. II. Chemical and mineralogical properties of HDPy-montmorillonite. *Appl. Clay Sci.* **2000**, *16*, 15–29.
(7) Heinz, H.; Vaia, R. A.; Krishnamoorti, R.; Farmer, B. L. Self-assembly of alkylammonium chains on montmorillonite: Effect of chain length, head group structure, and cation exchange capacity. *Chem. Mater.* **2007**, *19*, 59–68.
(8) Zhou, Q.; He, H. P.; Zhu, J. X.; Shen, W.; Frost, R. L.; Yuan, P. Mechanism of p-nitrophenol adsorption from aqueous solution by HDTMA(+)-pillared montmorillonite: implications for water purification. *J. Hazard. Mater.* **2008**, *154*, 1025–1032.
(9) Zhou, G. Z.; Zhou, L. C.; Li, Y. F.; Liu, X. X.; Ren, X. J.; Liu, X. L. Enhancement of phenol degradation using immobilized microorganisms and organic modified montmorillonite in a two-phase partitioning bioreactor. *J. Hazard. Mater.* **2009**, *169*, 402–410.
(10) Hata, H.; Mallouk, T. E.; Kuroda, K. Color tuning of acidic blue dye by intercalation into the basic interlay galleries of a poly(allylamine)/synthetic flouromica nanocomposite. *Chem. Mater.* **2009**, *21*, 985–993.
(11) Xi, Y.-F.; Frost, R. L.; He, H.-P.; Kloprogge, T.; Bostrom, T. Modification of Wyoming montmorillonite surfaces using a cationic surfactant. *Langmuir* **2005**, *21*, 8675–8680.
(12) Liu, R.; Frost, R. L.; Martens, W. N.; Yuan, Y. Synthesis, characterization of mono, di, and tri alkyl surfactant intercalated Wyoming montmorillonite for the removal of phenol from aqueous systems. *J. Colloid Interface Sci.* **2008**, *327*, 287–294.
(13) Zhu, J.-X.; Zhu, L.-Z.; Zhu, R.-L.; Tian, S.-L.; Li, J.-W. Surface microtopography of surfactant modified montmorillonite. *Appl. Clay Sci.* **2009**, *45*, 70–75.
(14) Madsen, F. T. Clay mineralogical investigations related to nuclear waste disposal. *Clay Miner.* **1998**, *33*, 109–129.
(15) Schecher, W. D.; McAvoy, D. C. MINEQL+: A chemical equilibrium modeling system, version 4.5 for Windows, User's manual, v2.00; Environmental Research Software: Hallowell, Maine, 2003.
(16) Dzombak, D. A.; Morel, F. M. M. *Surface Complexation Modeling: Hydrous Ferric Oxide*, Wiley-Interscience: New York, 1990.
(17) Tournassat, C.; Ferrage, E.; Poinsignon, C.; Charlet, L. The titration of clay minerals. II. Structure-based model and implications for clay reactivity. *J. Colloid Interface Sci.* **2004**, *273*, 234–246.
(18) Baeyens, B.; Bradbury, M. H. A mechanistic description of Ni and Zn sorption on Na-montmorillonite. 1. Titration and sorption measurements. *J. Contam. Hydrol.* **1997**, *27*, 199–222.
(19) Li, Z.-H.; Jiang, W.-T.; Hong, H.-L. An FTIR investigation of hexadecyltrimethylammonium intercalation into rectorite. *Spectochim. Acta A* **2008**, *71*, 1525–1534.
(20) Xu, L.-H.; Zhu, L.-Z. Structures of OTMA- and DODMA-bentonite and their sorption characteristics towards organic compounds. *J. Colloid Interface Sci.* **2009**, *331*, 8–14.
(21) Marras, S. I.; Tsimpliarak, A.; Zuburtikudis, I.; Panayiotou, C. Thermal and colloidal behavior of amine-treated clays: the role of amphiphilic organic cation concentration. *J. Colloid Interface Sci.* **2007**, *315*, 520–527.
(22) Perez-Santano, A.; Trujillano, R.; Belver, C.; Gil, A.; Vicente, M. A. Effect of the intercalation conditions of a montmorillonite with octadecylamine. *J. Colloid Interface Sci.* **2005**, *284*, 239–244.
(23) Ferrage, E.; Lanson, B.; Sakharov, B. S.; Dtits, V. A. Investigation of smectitie hydration properties by modeling experimental X-ray diffraction patterns: part I. Montmorillonite hydration properties. *Am. Mineral.* **2005**, *90*, 1358–1374.
(24) Lide, D. R., editor-in-chief. *Handbook of Chemistry and Physics*, 88th ed.; CRC Press, 2007−2008.
(25) Osman, M. A.; Ploetze, M.; Skrbal, P. Structure and properties of alkylammoniun monolayers self-assembled on montmorillonite platelets. *J. Phys. Chem. B* **2004**, *108*, 2580–2588.
(26) Cullity, B. D.; Stock, S. R. *Elements of X-ray Diffraction*, 3nd ed.; Prentice Hall: NJ, 2001.
(27) He, H.-P.; Frost, R. L.; Zhu, J.-X. Infrared study of HDTMA+ intercalated montmorillonite. *Spectrochim. Acta A* **2004**, *60*, 2853–2859.

ES100349K